

Cytoskeletal interactions with post-mitotic migrating nuclei in the oyster mushroom fungus, *Pleurotus ostreatus*: evidence against a force-generating role for astral microtubules

S. G. W. KAMINSKYJ, K. S. YOON* and I. B. HEATH†

Biology Department, York University, 4700 Keele Street, North York, Ontario M3J 1P3, Canada

*Present address: Department of Microbiology, Kangwon University, Chunchon 200, South Korea

† Author for correspondence

Summary

Nuclei of *Pleurotus ostreatus* migrate in a highly predictable manner following conjugate mitosis at clamp connections. Parameters were determined by observations in living hyphae and these data were used to predict the living behaviour of freeze-substituted nuclei. Three of four classes of nucleus migrate immediately after telophase and move at similar speeds. Freeze-substitution electron microscopy shows that these nuclei have prominent nucleus-associated organelles (NAOs) with large astral microtubule (MT) arrays. Although the NAOs do not have a consistent position with respect to the nuclear motion, they are preferentially located near the hyphal axis. The fourth class of nucleus remains in the developing clamp until it fuses with the main hypha, whereupon it migrates to its interphase position at a rate much faster than the

other classes. This class of nucleus has a small NAO and no astral MTs. Treatment of hyphae with a MT-disrupting drug, MBC, reduced the astral arrays in the first three classes but did not slow their rate of movement. Moreover, serial section analysis of drug-treated nuclei whose migration rate at the time of fixation was known showed no relationship, positive or negative, between astral MT number and rate of movement. These data suggest that astral MTs neither generate nor transduce force for post-mitotic nuclear migration in *P. ostreatus*. The role of astral MTs and possible mechanisms of post-mitotic nuclear migration are discussed.

Key words: cytoskeletal interactions, migrating nuclei, *Pleurotus ostreatus*.

Introduction

Eukaryotic cells possess systems for ensuring the correct positioning and movement of most organelles during various phases of cell development. A diversity of data has made it obvious that components of the cytoskeleton, especially microtubules (MTs) and actin filaments, are involved in some way in generating these movements, and recently a diversity of molecules such as dyneins, microtubule-associated proteins, myosin and kinesin have been added to the list of known participatory molecules. It is becoming clear that different organelles in different cells use different mechanochemical systems (e.g. see Adams and Pollard, 1989). Indeed, in a highly specialized organelle translocation system such as the axon, it appears that different mechanochemical molecules are used for the movements of a single organelle in opposite directions (e.g. see Adams and Pollard, 1989). Consequently, it is very difficult to predict from one cellular situation to another when investigating organelle motors, so each system must be analyzed individually.

In the fungi, one of the important types of movement is the migration of interphase nuclei. Within a single cell, the movements are generally intermittent, correlated with other cell cycle events, occur at diverse rates and occur in intimate association with the movements of other organelles. Consequently, bulk biochemical investigative techniques are impractical, genetic lesions in known molecules may fail to differentiate between primary and secondary effects, and genetic lesions giving useful phenotypes are not easy to attribute to a functional molecule (Meyer *et al.* 1988). For these reasons we have chosen to analyze nuclear motility using morphological techniques.

The morphological arrangement of moving nuclei and their associated cytoskeletal elements can differentiate between hypothetical models of movement and indicate possible mechanochemical components and control mechanisms. However, morphological data are only valid if they are based on the best available resolution, detectability and preservation of nuclei whose behaviour is accurately known. It is also vital to have three-dimen-

sional information about the motile nuclei so that observations can be categorized as normal, dominant or rare. At present the best high-resolution three-dimensional way of analyzing the morphology of cells in a state most close to life is by serial-section dissection of freeze-substituted cells. However, it is technically impossible to achieve satisfactory fast-freezing of cells undergoing observation at the time of fixation. Consequently, it is essential to have a highly predictable system so that the living behaviour of nuclei located in fixed material can be inferred with a high degree of certainty. The movements of nuclei following mitosis at clamp connections in basidiomycete hyphae offer such features. This is equivalent to the phase IV studied by Girbardt (1968) in *Trametes versicolor*. We have chosen to study this system in the oyster mushroom fungus, *P. ostreatus*, a species of considerable commercial value. We present results that show that microtubules are indeed involved in nuclear motility in *P. ostreatus* but not in expected ways.

Materials and methods

Monokaryotic cultures of *P. ostreatus* (Jacquin) Fries, numbers 42513 and 42514, were obtained from the American Type Culture Collection. They were co-inoculated onto Lu's modification (B. C. Lu, personal communication) of Brodie's (1949) nutrient agar. Lu's agar contained 5.0 g maltose, 2.0 g glucose, 2.0 g yeast extract, 1.6 ml glycerine, 0.2 g peptone, 0.5 g KH_2PO_4 , 0.5 mg MgSO_4 , 0.1 g $\text{Ca}(\text{NO}_3)_2$, 0.5 ml ferric citrate solution (2.7 g ferric citrate and 2.1 g citric acid in 100 ml distilled water), and 15 g Difco Bacto agar per litre of water. A dikaryotic culture was formed as shown by the development of clamp connections and thereafter the experimental stock was maintained as a dikaryotic culture on Lu's or YMG agar. YMG agar consisted of 0.4% Difco yeast extract, 1.0% Difco malt extract and 0.4% glucose per litre of distilled water solidified by 1.0% Difco Bacto agar.

Dikaryotic hyphae of *P. ostreatus* were grown for 3–5 days on Lu's or YMG agar at 22°C before experiments. For most observations of normal nuclear behaviour, and all inhibitor studies and freeze substitution or conventional fixations, hyphae were grown on dialysis membrane strips coated with 0.6% locust bean gum and overlain on agar. Some nuclear behaviour was also observed in hyphae grown on agar-coated slides covered with coverslips. Observations of living hyphae were made with a Reichert Polyvar microscope equipped with a $\times 100$ 1.25 NA phase-contrast objective and were recorded on videotape with time–date generated data superimposed. Measurements were made from the screen after calibration with a stage micrometer. Inhibitor studies with methyl benzimidazole-2-yl carbamate (MBC) were conducted in a flow-through chamber (Heath, 1988) whilst the cells were viewed and recorded with the above system.

For freeze substitution, hyphae were frozen, following minimal disturbance, in liquid propane, substituted in osmium tetroxide in acetone and flat-embedded in Spurr's resin as previously described (Meyer *et al.* 1988). For hyphae undergoing observation, the cells were fixed by perfusion of the flow-through chamber with 5% glutaraldehyde in 0.1 M-cacodylate buffer, pH 7.0. After fixation, low-magnification pictures were taken so that the treated hyphae could be re-located. The dialysis tubing with attached culture was carefully removed from the chamber and transferred to an embryo cup where the hyphae were fixed for 1 h in glutaraldehyde, washed with

cacodylate buffer, post-fixed with 1% OsO_4 for 1 h, dehydrated in an ethanol series, passed through acetone and embedded as above. Control conventionally fixed cultures were prepared entirely in embryo cups. Embedded cells showing the desired growth characteristics were individually selected with $\times 100$ phase-contrast optics, serially sectioned onto single-slot grids, stained in uranyl acetate and lead citrate, and examined and recorded with a transmission electron microscope.

In order to measure the number of nucleus-associated organelle (NAO)-associated (astral) microtubules, we placed reference lines at 0.5 μm ahead of or behind the centre of the NAO in exactly the same place in all serial sections through the NAO region of the nucleus. These lines were perpendicular to the long axis of the hypha. We counted the number of NAO-associated microtubules intersecting these lines. This procedure is simpler than attempting to track and thus precisely count all MTs (which is difficult to do in regions of high MT density) but is sufficiently accurate, since a longitudinally sectioned MT is likely to be contained in only one section at any point along its length. Because most astral MTs run approximately parallel to the long axis of the hypha, the transverse scoring lines intersected most but not quite all astral MTs.

In order to calculate the axial position of the NAOs, the distance between the centre of the NAO and plasmalemma was compared to the hyphal diameter. If a median longitudinal section of the hypha did not contain a median section of the NAO, the NAO–plasmalemma distance was measured, using section counting, assuming an average section thickness of 70 nm. The results were expressed as % deviation from the hyphal axis in such a way that 0% indicated an NAO exactly centered on the axis and 100% alignment on the plasmalemma.

Results

General behaviour of motile nuclei

Hyphae of *P. ostreatus* are comparable to those of many dikaryotic basidiomycete fungi in that the apical cell grows by tip extension with two closely spaced nuclei moving slowly forward with the growing hyphal tip until the cell is approximately 250 μm long. At this time the nuclei are close to the centre of the cell, a clamp connection forms and the two nuclei divide somewhat synchronously. After mitosis, two daughter nuclei move forward to approximately the centre of the apical cell while the other two move backward to a central position in the subapical cell. A septum forms across the main axis of the hypha to delimit the apical cell. This cycle is repeated continuously during colony growth.

In apical cells that have completed their post-mitotic migrations, described below, the two nuclei move at about the same rate as the tip grows ($0.96 \pm 0.55 \mu\text{m min}^{-1}$, $n=16$), so that they maintain a somewhat constant distance behind the apex. In hyphae at the margin of the colony, those used in this work, this distance was $105.7 \pm 19.2 \mu\text{m}$ ($n=17$, range 58.2–128.8 μm), measured from the nucleolus of the leading nucleus to the tip. Variations in cell length, largely determined by the extent of tip growth following septum formation, are accommodated by considerable variability in the distance between the nuclei (measured from the midpoint between the two nuclei) and the septum (mean $143.5 \pm 68.7 \mu\text{m}$, $n=17$, range 43.2–285.3 μm).

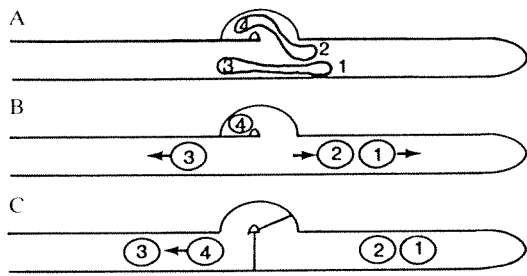


Fig. 1. Schematic representation of nuclear movements during conjugate mitosis in *P. ostreatus*: A, the nuclei complete mitosis approximately synchronously, one in the clamp and the other in the main hypha; B, immediately after telophase, N1, N2 and N3 begin to migrate toward their interphase positions; N4 remains in the developing clamp; C, after the clamp fuses with the main hypha, N4 migrates to its interphase position beside N3.

Conjugate mitosis in *P. ostreatus*

Following the initiation of clamp connection formation, one nucleus moves into the clamp prior to undergoing mitosis whereas the other completes mitosis in the main hypha (Fig. 1A). During and immediately after telophase one daughter nucleus from each mitosis rapidly moves forward, i.e. towards the hyphal tip. We designate these as N1 and N2 (Fig. 1B). The other daughter nucleus from the mitosis in the main hypha (designated N3) moves rapidly backward at about the same time (Fig. 1B). The fourth nucleus (designated N4) remains in the clamp for some time until the tip of the clamp fuses with the main hypha at which time it moves backward (Fig. 1C). The positions of the four nuclei with respect to each other and to the clamp as well as their direction of migration are defined unambiguously by their assigned number.

Two septa form synchronously during conjugate mitosis. The septum across the main hypha forms prior to clamp fusion with the main hypha and it is the site relative to which all nuclear migrations are measured. Its position with respect to the clamp is highly predictable so that measurements were accurate even before visible septum formation. The septum across the clamp is of no consequence to this work.

In interphase nuclei the nuclear envelope is distinguishable; the nucleoli are very clear and they are the most easily monitored part of the nucleus. However, during mitosis both the nuclear envelope and the nucleolus become indistinct, so that nuclear division and very early nuclear migration cannot be monitored accurately. Disappearance of the nucleoli from nuclei lying beside a developing clamp connection marks the beginning of mitosis at the light-microscope level and is the time relative to which all drug treatments were calculated. The nucleoli re-form at an early stage in post-mitotic migration and then it becomes possible to track nuclear movements accurately.

Post-mitotic nuclear migratory behaviour

Representative post-mitotic nuclear migratory behaviour is illustrated in Figs 2 and 3. Three of the four classes of

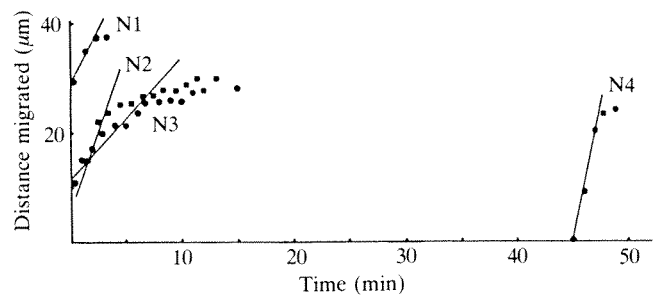


Fig. 2. Post-mitotic migratory behaviour of *P. ostreatus* nuclei showing an initial rapid migration phase followed by slower movement as the interphase position was approached. The migration rate, the slope of the lines, was always calculated from the rapid phase if one were detected. N1–N3 migrate immediately after telophase, much sooner and more slowly than N4.

daughter nuclei, N1, N2 and N3, migrate immediately after mitosis. We determined the migration rate for each nucleus by plotting distance from the septum to the nucleolus *versus* time. Most commonly, nuclei show a rapid migration phase followed by slower movement as they approach their interphase position (Fig. 2). However, this rapid phase was not always observed (Fig. 3) and its lack did not clearly correlate with either time or distance migrated at the earliest observation. The mean migration rates were calculated from the slope of the best-fitting line but the nuclei did not always move smoothly; periods of more rapid travel were interspersed with periods of slower motion even within the fast or slow migration phases, although within either phase the variations were not dramatically different from the mean and complete stops were never observed. Because many

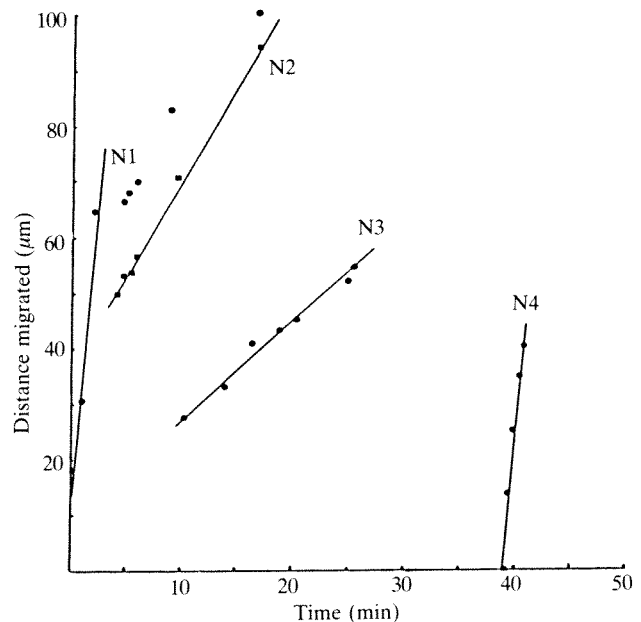


Fig. 3. Post-mitotic nuclear migratory behaviour of four nuclei, three (N2–N4) of which did not show an initial rapid migration. N1–N3 migrated at similar speeds, much slower and sooner after telophase than N4.

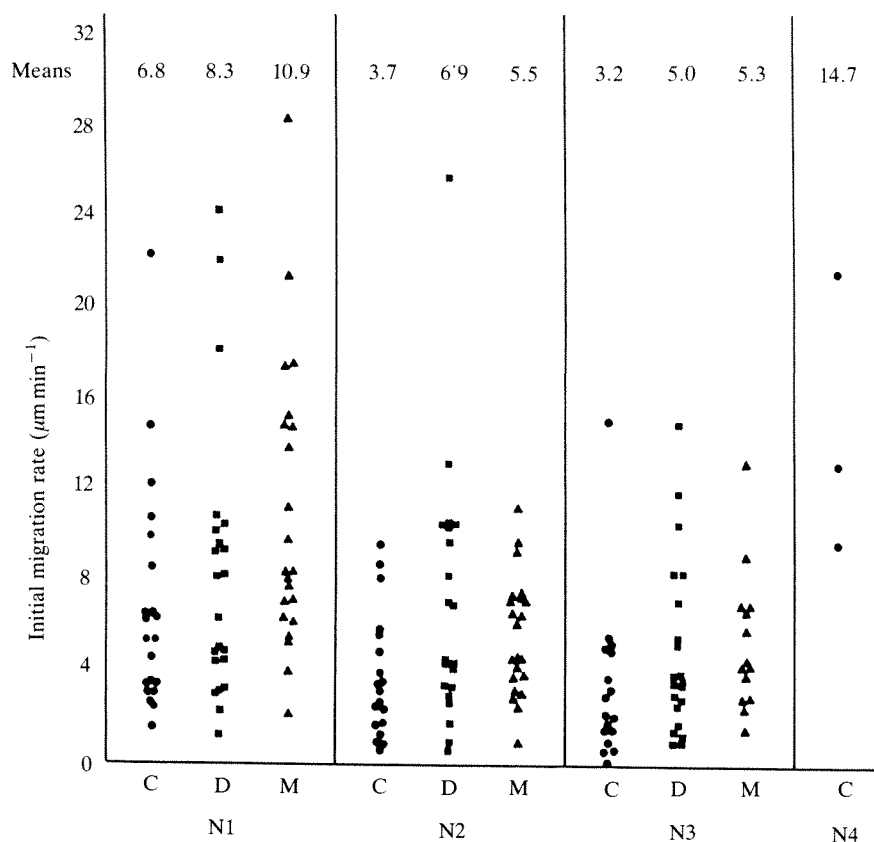


Fig. 4. Initial rates of migration for untreated control (C), DMSO-treated (D) and MBC/DMSO-treated (M) living N1–N4 nuclei. The number at the top of each column gives the mean migration rate for that column. Analysis of the control data only by ANOVA and Tukey test shows $N1=N2=N3$, and $N1, N2, N3 \neq N4$. Analysis of the same data by ANOVA and Newman-Keuls test shows $N1 \neq N2, N3, N4$; $N2=N3$; $N4 \neq N1, N2, N3$. Analysis of all treatments of N1–N3 by ANOVA shows that there is no significant difference between treatments.

nuclei showed a bimodal migration pattern, calculating an overall rate of movement was not meaningful as such a rate would be strongly influenced by the length of time that the nucleus was tracked. We therefore chose to compare the initial rates of migration for all nuclei, whether or not a bimodal migration pattern was detected.

Differential classes of nucleus migrate at different speeds (Fig. 4). A comparison of the rates among N1, N2 and N3 showed that the significance of differences depends partially on which statistical test was used. As a group these three nuclei moved much more slowly than N4. N4 remains trapped in the developing clamp connection until the tip of the clamp fuses with the hypha, after which it migrates rapidly to its interphase position anterior to N3. Because the migration of N4 is delayed and then is very brief and because prolonged illumination of the clamp even at low light intensities inhibits N4 migration, this event was seldom observed.

In order to predict the motile behaviour of nuclei, it is necessary to know both the rate of movement and the distance moved. The distances moved by the nuclei are shown in Fig. 5. Because we did not obtain complete analyses of all moving nuclei, the average distances moved are only minimum estimates. For the subsequent parts of this work the important distance parameters are the estimates of the likelihood of a nucleus located at a specific distance from the septum showing post-mitotic migration. These estimates are given in Fig. 5. The combined speed and distance data give us an indication of the probable pre-fixation behaviour of any nucleus, based

on its relationship to the septum in fixed and embedded hyphae.

Morphological features of freeze-substituted migrating nuclei

We examined a total of 11 freeze-substituted nuclei whose probability of being moving at the time of fixation was between 82 and 100%, based on their distances from the septum and the data in Fig. 5. The characteristics of these nuclei are given in Table 1.

The NAOs of migrating freeze-substituted nuclei were prominent, large and fibrous (Fig. 6). Although obviously associated with the nucleus, they were not tightly appressed to the nuclear envelope and there was not always an associated, detectable, intranuclear structure. The NAOs of migrating nuclei were associated with vesicles of unknown function, interspersed between the astral MTs (Fig. 6, inset).

The NAOs of migrating nuclei lie at the focus of extensive astral MT arrays (Figs 6 and 7). These astral MTs end close to the fibrous NAO material but do not penetrate it. They extend as cones both ahead of and behind the migrating nucleus when analyzed through serial sections (Fig. 7). Ahead and behind are always with respect to the direction of nuclear motion and are therefore opposite in absolute direction when referring to N1 and N2 *versus* N3 and N4. Although our data were incomplete for some nuclei, it was clear that there was no significant difference in the number of astral microtubules emanating ahead of and behind the N1–N3

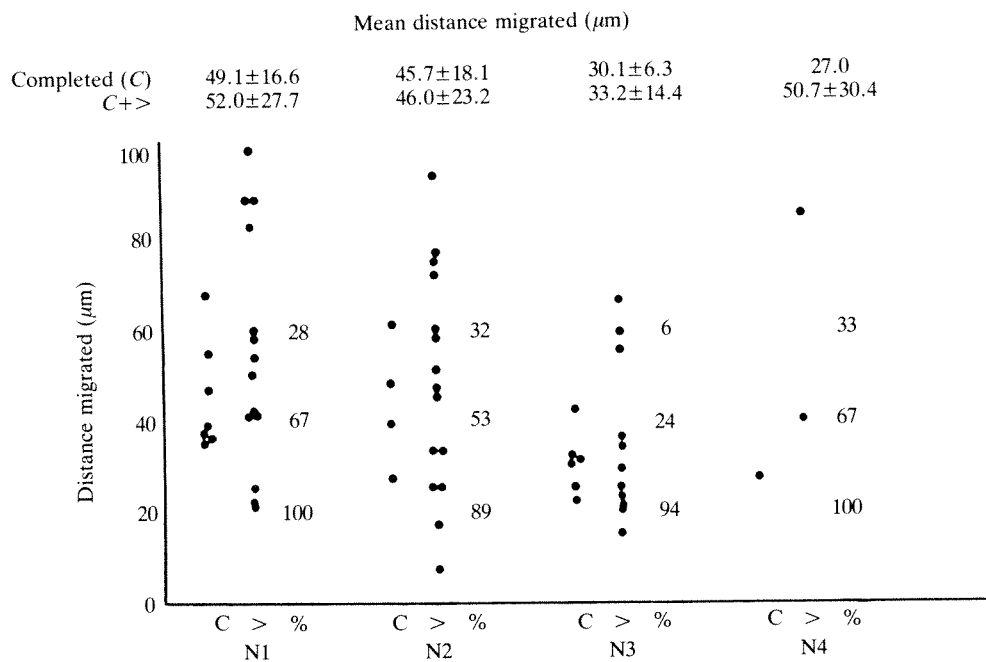


Fig. 5. Distances migrated by post-mitotic nuclei of *P. ostreatus*. It was not possible to obtain complete migration data on all nuclei. Therefore, records are divided into those where the nuclei had slowed to hyphal growth rates (C) and those that had not (C+>) at the time observation ceased. The numbers in the % columns show the percentage of observed nuclei that migrated past the indicated distance, given at 20- μm increments. These are minimum estimates because they include nuclei that were travelling when the observation ceased. These values indicate the probability of a nucleus at any different position being in motion.

nuclei (means 20.0 ± 7.9 ahead versus 19.9 ± 7.7 behind, $n=9$). Overall, 54.2% of astral MTs radiated ahead of the nuclei. Cytoplasmic MTs in *P. ostreatus*, both astral and non-NAO-associated, are often long ($>16 \mu\text{m}$) and undulating. It was possible to track many, but not all, to their ends to determine if they terminated at the plasmalemma (defined as positively ending within 100 nm of that membrane). In a population of 43 astral MTs associated with four migrating nuclei, only 2% were associated with the plasmalemma. In contrast, 60% of a group of 47 astral MTs emanating from the two poles of a metaphase nucleus were associated. We were also able to track to

both ends 25 non-NAO-associated MTs that skimmed the nuclear envelopes of migrating nuclei in one hypha. Of these, 24% were associated with the plasmalemma, and frequently ran parallel to it for several micrometres. A third class of cytoplasmic MTs, apparently not associated with nuclei, were frequently seen running parallel to the plasmalemma for long distances but we have not followed these in detail.

The position of the NAO with respect to the migrating nucleus was variable. Since the nuclei always migrate in a predictable direction with respect to the clamp this relationship can be known unambiguously for nuclei in

Table 1. Characteristics of analyzed nuclei

Treatment	Hypha	N1				N2				N3				N4				
		D	P	MT+	MT-	D	P	MT+	MT-	D	P	MT+	MT-	D	P	MT+	MT-	
Freeze substitution	A	34	86	17+	13+	15	95	25+	25+	14	100	17+	14+	-	-	-	-	-
	B	32	86	13+	11+	23	89	9+	7+	20	94	15+	10+	-	-	-	-	-
	C	21	100	21	24	14	95	32+	29+	23	53	31+	19+	-	-	-	-	-
	L	-	-	-	-	-	-	-	-	-	-	-	-	-	15	100	0	0
	M	-	-	-	-	-	-	-	-	-	-	-	-	-	14	100	0	0
	N	65	28	0	0	55	37	0	0	-	-	-	-	-	-	-	-	-
Conventional fixation	D	32	86	17	17	12	95	25	43	13	100	26	35	-	-	-	-	-
DMSO-conventional fixation	E	38	67	17	10	30	74	16	7	24	76	10	8	-	-	-	-	-
MBC/DMSO-conventional fixation	F	54	43	4	1	41	58	7	6	36	29	16	7	-	-	-	-	-
	G	25	90	2+	1+	5	100	5	7	16	94	1+	3+	-	-	-	-	-
	H	47	47	4	2	19	89	3+	3+	16	94	0+	6+	-	-	-	-	-
	I	58	33	3	3	33	74	3	7	18	94	4+	5+	-	-	-	-	-
	J	36	76	10	7	18	89	8	8	18	94	6	1	-	-	-	-	-
	K	39	67	6	1	15	95	8+	8+	18	94	5+	8+	-	-	-	-	-

Migration and microtubule characteristics for the nuclei used in the EM portion of this study. The distances migrated (D) were measured from montages of median sections. The probabilities (P) of individual nuclei being in motion at the time of fixation are calculated from the data shown in Fig. 5. Because those values include nuclei that were still moving at the end of the observation period, the probabilities given in this table are minimum estimates. However, for hyphae E-K, the nuclei were being observed at the time of their fixation, and therefore were known to be moving. The numbers of microtubules leading (MT+) and trailing (MT-) the nuclear motion were determined using serial sections through the NAO-containing region as described in Materials and methods. The '+' after some data indicates that complete information was not available. However, considering the available information, and assuming that equal numbers ahead of and behind the NAO were missed, MT+ and MT- were not significantly different (*t*-test, $P < 0.05$).

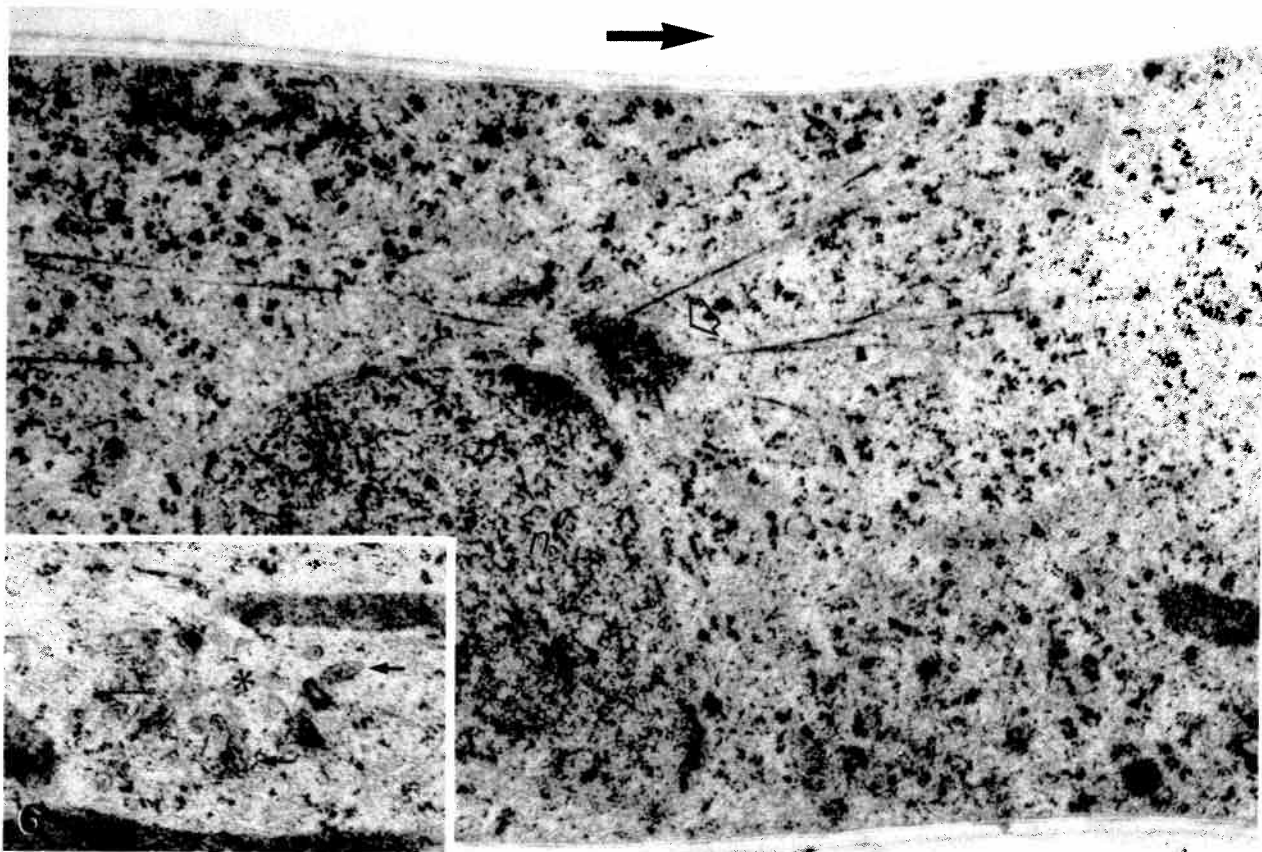


Fig. 6. One of a series of sections through the NAO (open arrow) of nucleus C2 (see Fig. 8) showing its fibrous nature and that it lies at the focus of a microtubule array that extends predominantly ahead of and behind the nucleus (*n*). The direction of migration is given by the large arrow. The radial position for this NAO is 33%. $\times 44\,460$. Inset: section close to the surface of an NAO (position marked by asterisk), showing the vesicles (small arrows) that are commonly interspersed between the astral MTs of migrating nuclei. $\times 27\,360$.

fixed material. Tracings from serial sections of both freeze-substituted and conventionally fixed nuclei with their NAO positions indicated (Fig. 8) show that the NAO–nucleus relationship is independent both of nucleus class (i.e. N1 *versus* N2, etc.) and of the individual hypha. Of the 11 nuclei analyzed in this manner, 14% had the NAO at the absolute front of the nucleus with the distribution of the others shown in Fig. 8.

Although the position of the NAO was variable with respect to the migrating nucleus it was remarkably constant with respect to the radius of the hypha. The location of the centre of the NAO was calculated relative to the centre of the hypha such that 100% referred to an NAO centered on the plasmalemma (clearly an impossibility) and 0% to an NAO positioned exactly in the middle of the hypha. Among 11 migrating freeze-substituted N1–N3 nuclei, the position of the NAO was $20 \pm 7\%$, i.e. close to the centre of the hypha.

Freeze-substituted migrating nuclei often had prominences that were not related to the position of the NAO (Fig. 8). The prominences were smoothly contoured and not acutely pointed. Cytoplasmic MTs that skimmed the nuclear envelope were occasionally seen adjacent to these prominences but were not always present.

Serial sections of migrating N4s revealed that their NAOs were much smaller than those of other nuclei (Fig. 9) and did not have MTs emanating from them. The N4 NAOs closely resemble those of non-migrating nuclei (Fig. 10). Migrating N4s were associated with cytoplasmic MTs that skimmed their envelopes (Fig. 9). The radial position of the migrating N4 nuclei also differed from those of N1–N3, being more peripheral at 74% for two nuclei compared to 75% for two non-migrating N1–N3 nuclei.

Effects of MBC on nuclear migration

Because cytoplasmic microtubules are often implicated in nuclear mobility, we sought to investigate their role in *P. ostreatus* by disrupting them with MBC. Selecting the optimal concentration and time of application of MBC was difficult: too much or too soon inhibited mitosis and, consequently, secondarily completely blocked post-mitotic migration. Too little or too late, and migration was completed before the drug could penetrate and elicit an effect. This rather delicate balance undoubtedly explains at least part of the variability encountered in our results. However, preliminary experiments showed that perfusion of hyphae in a flow-through chamber with $50\ \mu\text{M}$ -

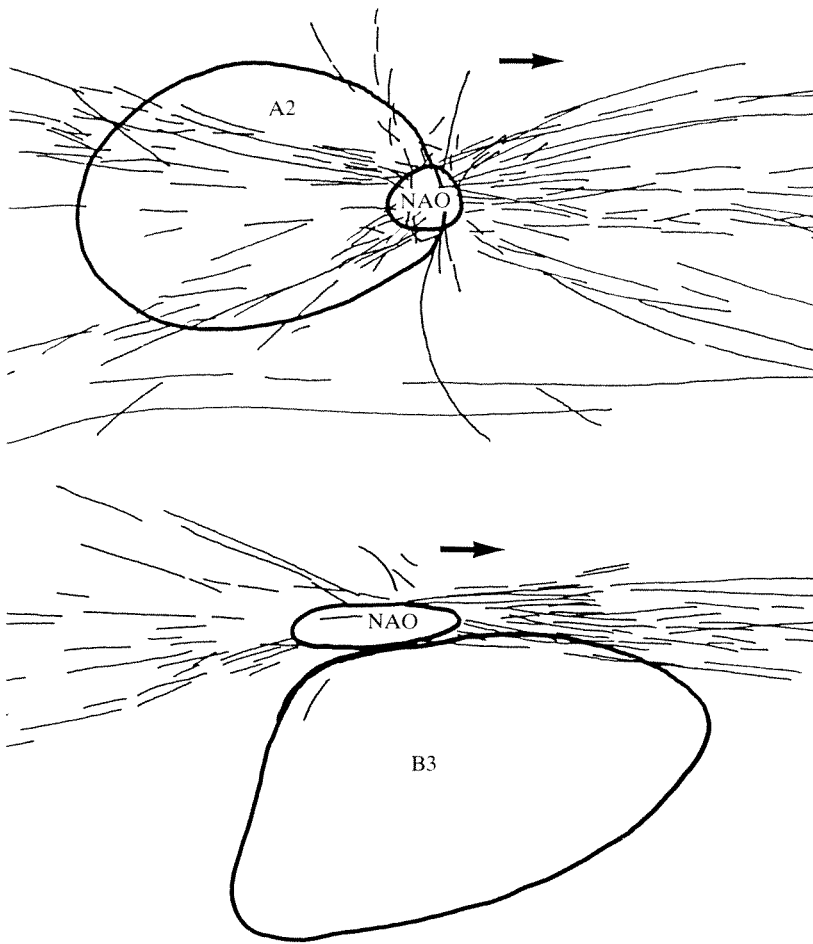


Fig. 7. Tracings of near-median sections of two migrating freeze-substituted nuclei indicating the NAO plus astral and associated microtubule arrays. The direction of migration is to the right as indicated by the arrows. The characteristics of the nucleus can be found by referring to the identification numbers in Table 1 and Figs 8 and 11. Each reconstruction is from the same series of sections used to obtain the data in Table 1, consequently the numbers can be compared directly.

Treatment	Morphology of migrating nuclei				Hypha	
	Hypha	N1	N2	N3		N4
Freeze substitution (FS)	A					L
	B					M
	C					
Conventional fixation (CF)	D					
	E					
DMSO-CF	F					
	G					
MBC/DMSO-CF	H					
	I					
	J					
	K					
		l	a	m	p	
FS		4	3	3	1	
CF		1	1	0	1	
DMSO-CF		0	3	2	1	
MBC/DMSO-CF		0	6	6	3	
Total		5	13	11	6	
%		14	37	31	17	

MBC in 0.5% dimethyl sulphoxide (DMSO) (hereafter simply called MBC) in culture medium at 2 min after the dispersal of the nucleolus (which marked the beginning of mitosis at the light-microscope level) were the highest concentration and the earliest time that did not inhibit completion of karyokinesis or nuclear migration. Thus these conditions were used in all subsequent experiments.

We were not able to effect complete elimination of astral MTs with MBC during the critical phase of nuclear migration. However, we were able to reduce substantially their numbers relative to both control and DMSO-treated nuclei from a mean of 40.2 in controls to 16.3 with

Fig. 8. Tracings of median sections of the migrating nuclei used in the EM study. All nuclei are drawn moving to the right, as indicated by the large arrow. Each nucleus can be unambiguously identified by upper case letter (hypha) and number (nuclear class) and these identifications are used in Figs 11 and 12 and in Table 1. The N4 class of migrating nuclei were not found in the same hyphae as the other nuclear classes, hence their different letters. The filled patches indicate the position, shape and relative size of the NAOs. The lower case letters refer to the position of the NAO relative to the nucleus: leading (l), anterior third (a), median third (m), and posterior third (p). There was no consistent difference in NAO position between treatments, hyphae or class of nucleus. These data are compiled at the bottom of the figure.

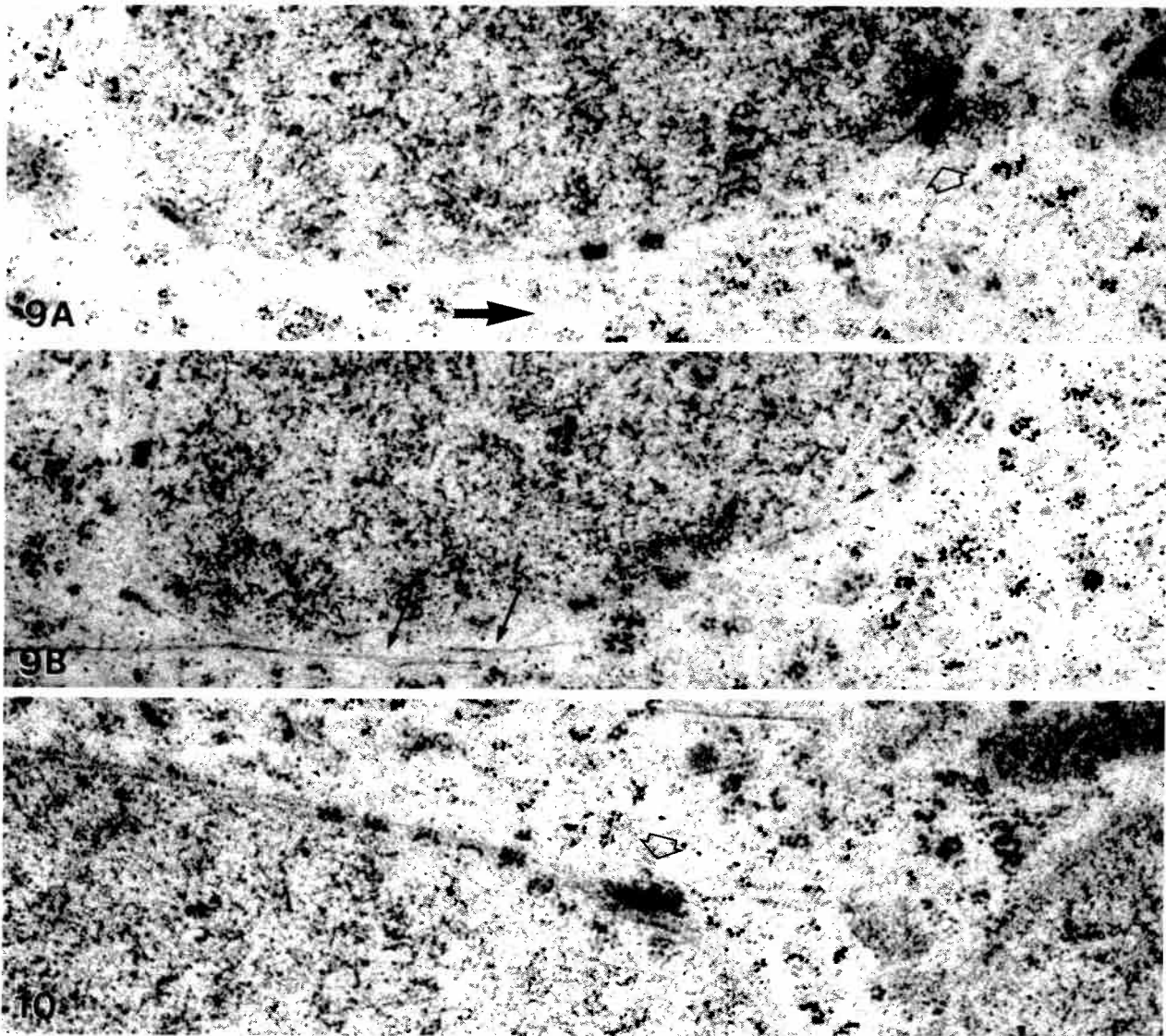


Fig. 9. Two sections (the two intervening sections are not shown) from a series through nucleus L4, which was migrating in the direction of the large arrow. A. The NAO (open arrow) is very much smaller and more condensed than is seen for the other classes of migrating nucleus (compare with Fig. 6) and resembles that of a non-migrating nucleus (compare with Fig. 10). There are no astral microtubules or associated vesicles. B. A pair of microtubules that are not associated with the NAO skims the nuclear envelope (small arrows). $\times 44\,460$.

Fig. 10. The NAO (open arrow) of a non-migrating N2 nucleus that has reached its interphase position adjacent to N1. The NAO is much smaller than for migrating nuclei of this class, but resembles that of a migrating N4 (compare with Fig. 9A). $\times 44\,460$.

DMSO and 9.3 with MBC. At a level of $P < 0.01$, MBC numbers were significantly lower than controls but neither differed significantly from the DMSO value. However, further analysis of the number of astral MTs showed that there was a general trend for their numbers to decrease with distance of migration (Fig. 11). With this factor considered, the MBC-attributable reduction in astral MTs is greater than seems apparent for the mean values (Fig. 11). Consequently, we conclude that MBC does indeed reduce the numbers of astral MTs associated with migrating nuclei. This same treatment does *not* reduce the rate of migration, instead it seems to cause a slight *increase* in rate (Fig. 4). However, this increase is

insignificant relative to DMSO. Both DMSO and MBC rates are higher than the control values, but we have not determined whether this apparent difference is due to the differences in obtaining data (agar cultures for controls *versus* flow-through cultures for DMSO and MBC) or reflects a real acceleration caused by the DMSO. The important point is that an MBC treatment that reduces the numbers of astral microtubules produces a slight increase, or at worst no change, in the rate of migration. This independence between number of MTs and migration rate is also shown by a direct comparison between the measured rate at the time of fixation and the subsequently recorded number of astral microtubules

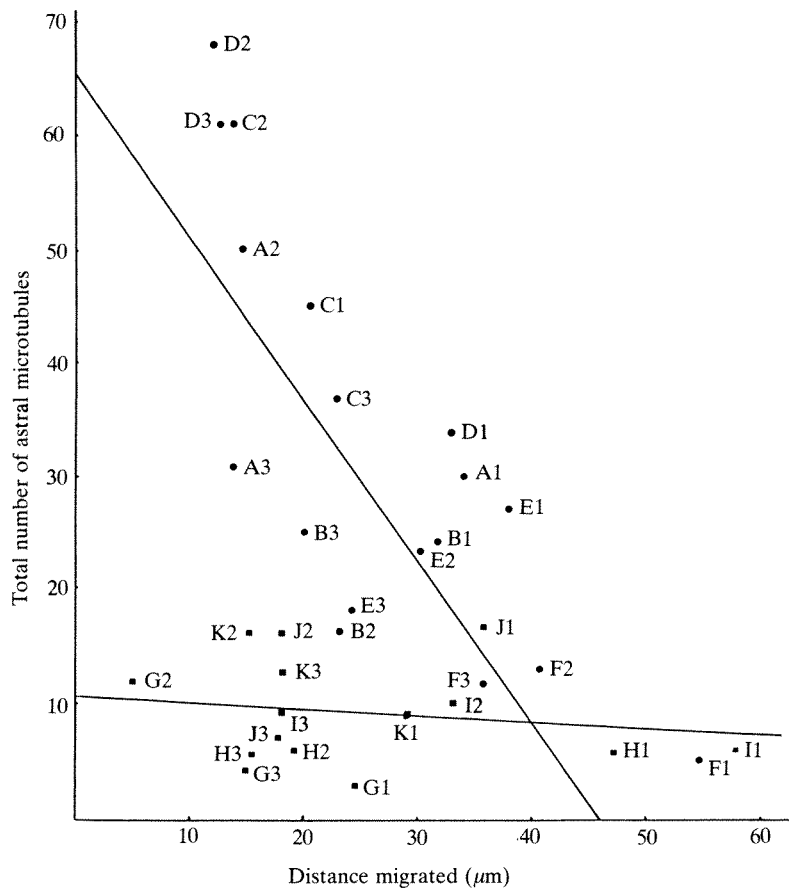


Fig. 11. Total number of astral MTs *versus* distance migrated for freeze-substituted, conventionally fixed or DMSO-treated conventionally fixed (●) and for MBC/DMSO-treated conventionally fixed nuclei (■). The linear regression lines for the two populations are shown. The microtubule numbers were counted from serial sections assessed at 0.5 μm ahead of and behind the centre of the NAO. Distance migrated by individual nuclei was measured from montages of median sections.

associated with those same nuclei (Fig. 12). These two parameters appear to be independent, some of the fastest movers had the lowest numbers of MTs and *vice versa*.

When we compared the positions of the NAOs, with respect to the migrating nuclei, of the 15 MBC-treated N1–N3 nuclei, none had a leading NAO and there were fewer (40% *versus* 64%) in the anterior third of the nucleus relative to the freeze-substituted controls (Fig. 8), but with relatively small sample sizes it is not clear whether these differences are significant. On these NAOs a mean of 48.3% of the astral MTs radiated forward, a value very similar to the 54.2% for the freeze-substituted controls mentioned previously. Overall, when we compared the number of leading *versus* trailing astral MTs for all of the 33 nuclei shown in Fig. 8, the

mean proportion leading was 52.4%. There were no significant differences in this respect when we compared nuclei N1, N2 and N3 or leading, anterior, median or posterior NAOs. Furthermore, the total number of astral MTs did not appear to differ between freeze substitution and conventional fixation (35.6 ± 14.5 , $n=9$ *versus* 54.3 ± 17.9 , $n=3$, respectively), although our sample sizes are again very low (Fig. 8).

When the radial relationship of the migrating, drug-treated NAOs was determined, the NAO position for the DMSO-treated nuclei was similar to the freeze-substituted hyphae at $14.1 \pm 12.7\%$ ($n=6$) but the positions of the MBC-treated hyphae were significantly different from either. The NAOs of MBC-treated nuclei were more variably positioned than the other treatments and

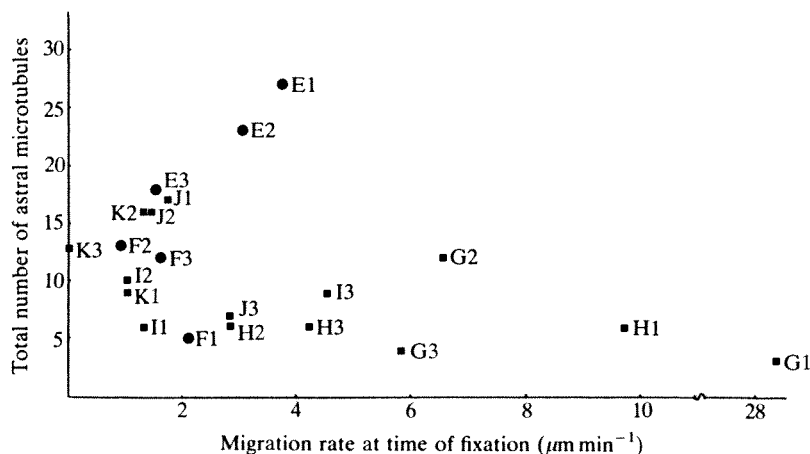


Fig. 12. Total numbers of astral MTs for DMSO-treated (●) or DMSO/MBC-treated (■) nuclei *versus* speed of migration at the time of fixation. The correlation coefficient for a linear regression is 0.367.

were more likely to lie between the nucleus and the closest plasmalemma than otherwise; their position was $47 \pm 24\%$ (range 18–92%, $n=15$).

The NAOs of migrating nuclei were also associated with small, vesicle-containing vacuoles of unknown function, interspersed amongst the MTs (Fig. 6). These vesicles were associated with migrating nuclei from all treatments and were occasionally present near mitotic NAOs.

The freeze-substituted migrating nuclei, although smooth in profile, often had prominences (Fig. 8) that were not associated with their NAOs. Migrating nuclei that had been treated with DMSO or MBC also had prominences, but these were much more acutely pointed. One DMSO-treated hypha had a nucleus that had had a small portion of its nucleus completely blebbed off as proven through serial sections. The DMSO- and MBC-treated nuclei occasionally had more than one of these finger-like projections per nucleus and they were seen both leading and trailing the nuclear motion.

The mitochondrial morphology of DMSO- and MBC-treated hyphae was strikingly different from that of control hyphae, whether conventionally fixed or freeze-substituted. Normal mitochondria are long flexuous cylinders of relatively constant diameter, but those in both DMSO- and MBC-treated hyphae were flattened in the middle with bulbous ends. Because control conventionally fixed mitochondria were similar to those prepared by freeze substitution, this morphological alteration was not a fixation artefact. The mitochondrial changes were induced by the DMSO within 12 min.

Discussion

By exploiting a system with a highly predictable pattern of nuclear behaviour, we have been able to utilize the optimal preservation and resolution associated with freeze-substitution and have combined this with conventional-fixation analysis of nuclear behaviour of nuclei whose behaviour in life could be correlated with aspects of their ultrastructure. Adding to these techniques with an anti-MT drug (MBC) and using serial section-based quantitative electron microscopy we have been able to achieve a more complete analysis of a fungal nuclear motility system than has been previously reported.

Previous analyses of fungal nuclear motility have tended to emphasize the potential force-generating role of the NAO-associated astral MTs (e.g. see Aist, 1969; Aist and Berns, 1981; Ashton and Moens, 1982; Byers and Goetsch, 1975; Girbardt, 1968; Hasek *et al.* 1987; Heath, 1981; Heath *et al.* 1982) although a contribution from non-astral cytoplasmic MTs seems likely according to other studies (Heath and Heath, 1978; McKerracher and Heath, 1985, 1986; Meyer *et al.* 1988, Raudaskoski and Koltin, 1973).

The extensive and prominent arrays of astral MTs associated with the migrating nuclei of *P. ostreatus* intuitively seem good candidates as force producers/transducers in this system but numerous aspects of our data argue against this possibility as follows: (1) the

consistently and dramatically faster rate of migration of N4 relative to N1–N3 occurs in a total absence of astral MTs. (2) If force were generated, or transmitted, by the astral MTs, it would be applied to the nucleus *via* the NAO, which would in turn predict that the NAO should consistently lead the migrating nuclei. This was not observed. (3) On the basis of what has been found in other cells, microtubules are polarized structures and the force-generating molecules such as dynein and kinesin function predominantly unidirectionally with respect to this polarity (Pratt, 1989). In other cells, astral microtubules have a uniform polarity (Heidemann and McIntosh, 1980), which suggests that those of *P. ostreatus* that run in equal abundance anteriorly and posteriorly must either be approximately 50% redundant (i.e. either anterior or posterior array non-functional) or that the two 'motors' must be coordinated, one to pull and the other to push. This seems unnecessarily complex and therefore an intuitively unlikely and non-parsimonious situation. (4) MBC treatment reduces the number of astral MTs with either no effect or a slight increase in the rate of migration. If astral MTs were motors or force transmitters, MBC should slow or stop migration. The independence between astral MT number and migration rate (Fig. 12) supports a similar argument. For these reasons, we conclude that astral MTs neither generate nor transmit the forces necessary to move the nuclei during post-mitotic migration.

However, some aspects of our data are contrary to this conclusion. For example, the decay in numbers of astral MTs with distance migrated approximately correlated with the two phase migration rates shown by some, but not all, nuclei, so that the slower phase could be attributed to the reduced number of MTs. Because of the variability in rates and numbers we cannot make a tight correlation here; this could only be done if it were possible to visualize the MTs associated with the living nuclei. However, the independence between astral MT number and migration rate referred to in aspect (4) above shows that there is no tight correlation.

We suggest that the declining numbers reflect a general depolymerization following mitosis. We further suggest that the astral MTs are important for force generation during mitosis but that following mitosis there is a time-dependent depolymerization. Consequently, the astral MTs present during migration are viewed as remnants with no function. Rather, they seem to retard movement, on the basis of the higher rates shown by the N4 nuclei and the MT-depleted MBC-treated nuclei. Observations consistent with this concept are the total absence of astral MTs on the N4 nuclei at the time of their migration. Remember that the N4 nuclei do not begin to migrate until some 30–40 min after mitosis compared with N1–N3, which go immediately. Furthermore, at mitosis a high percentage of the astral MTs associate with the plasmalemma, as suggested for force production during anaphase B–telophase in *Fusarium*, by Aist and Berns (1981), whereas this number drops considerably to negligible levels during migration. This is consistent with a role change. Similarly consistent is the change in the position of the NAOs, from the poles of the elongating

nuclei at mitosis where they would be expected if force were being applied *via* them to the nucleus, to various typically non-leading positions during migration. Their position during migration is presumably a chance function of the balance between force applied (perhaps intermittently; Aist and Bayles, 1988) elsewhere on the nucleus and drag on the NAOs and their associated MTs.

Thus we conclude that the astral MTs probably are force-generating or -transmitting during mitosis, as postulated by Aist and Berns (1981) and others (reviewed by Heath, 1981), but that they relinquish such a role during nuclear migration. Their presence at that time is simply an indication of the time needed for their depolymerization to result in an absence at interphase. Why it should take so much longer for the astral MTs to depolymerize than the spindle MTs, which depolymerize much earlier, is unclear; obviously different cellular locations (and thus possible ionic and MT subunit concentrations) or different microtubule-associated proteins could provide plausible explanations.

There is one feature of NAO behaviour during migration that is unexplained by the above conclusion. Normally the NAOs are very consistently centrally located in the hyphae whereas MBC causes them to become more randomly located. This implies some MT control over NAO position, which remains unexplained. Interestingly, this is the converse of the situation recently described in oomycete hyphae where the centrioles, which are NAO equivalents, are preferentially peripherally located (Heath and Kaminskyj, 1989).

Since astral MTs appear not to be involved in force production for nuclear migration, what is involved? One obvious candidate is the population of non-astral MTs that associate laterally with the nuclear envelopes. Similar MTs have been seen associated with other migrating nuclei (e.g. see Heath and Heath, 1978; McKerracher and Heath, 1985; Meyer *et al.* 1988; Raudaskoski, 1984; Raudaskoski and Koltin, 1973), so they appear to be a consistent feature of migrating nuclei, especially in basidiomycetes. If they are responsible for generating or transmitting the force, our data provide some indication of a likely mechanism. McKerracher and Heath (1985, 1986) proposed that similar cytoplasmic MTs interacted with unidentified (possibly a diffuse actin gel) components of the general cytoplasm. Conversely, Aist and Berns (1981) suggested that the astral MTs involved in mitotic movements interacted with the plasmalemma. Because only 24% of the nuclear envelope-associated MTs closely approach the plasmalemma in *P. ostreatus* we favour the McKerracher and Heath (1985, 1986) model. However, there is another very likely candidate for force application to the nuclear envelope and that is actin. In common with most studies of fungi, even freeze substitution fails to reveal an extensive array of actin in the cytoplasm, yet there is ample evidence for its abundance in various forms in a number of species (Adams and Pringle, 1984; Allen and Sussman, 1978; Anderson and Soll, 1986; Heath, 1987, 1988; Hoch and Staples, 1983; Runeberg *et al.* 1986; reviewed by McKerracher and Heath, 1987). Clearly some element, intra- or extranuclear, is capable of producing the nuclear pro-

trusions that occur even in freeze-substituted nuclei but more abundantly following DMSO or MBC treatments (Fig. 8). MTs are not typically associated with the projections. The increased prominence of the projections following DMSO treatment, which, at higher concentrations, is known to alter actin behaviour in other cells (Fukui, 1978, 1980; Fukui and Katsumaru, 1979, 1980; Sanger *et al.* 1980), is consistent with a role for actin in their generation, but at present we lack more definitive evidence for this hypothesis. However, if actin is indeed capable of generating the nuclear projections, it is an obvious candidate for generating overall mobility. In support of this suggestion, perinuclear actin has been demonstrated for *Neozygites* (Butt and Heath, 1988) and for *Saprolegnia* (review by Heath, unpublished). A role for actin and myosin in organelle motility has been shown by Adams and Pollard (1986). This hypothesis can only be fully evaluated when we have better methods for accurately describing the finest and most unordered actin arrays in cells.

This work was supported by an NSERC International Scientific Exchange Award for K.S.Y. and an NSERC Operating Grant to I.B.H.

References

- ADAMS, R. J. AND POLLARD, T. D. (1986). Propulsion of organelles isolated from *Acanthamoeba* along actin filaments by myosin-I. *Nature, Lond.* **322**, 754–756.
- ADAMS, R. AND POLLARD, T. D. (1989). Prediction of common properties of particle translocation motors through comparison of myosin-I, cytoplasmic dynein, and kinesin. In *Cell Movement*, vol. 2: *Kinesin, Dynein, and Microtubule Dynamics* (ed. F. D. Warner and J. R. McIntosh), pp. 3–10. New York: Alan R. Liss, Inc.
- ADAMS, A. E. M. AND PRINGLE, J. R. (1984). Relationship of actin and tubulin distribution to bud growth in wild-type and morphogenetic mutant *Saccharomyces cerevisiae*. *J. Cell Biol.* **98**, 934–945.
- AIST, J. R. (1969). The mitotic apparatus in fungi: *Ceratocytis fagacearum* and *Fusarium oxysporum*. *J. Cell Biol.* **40**, 120–135.
- AIST, J. R. AND BAYLES, C. J. (1988). Video motion analysis of mitotic events in living cells of the fungus *Fusarium solani*. *Cell Motil. Cytoskel.* **9**, 325–336.
- AIST, J. R. AND BERNS, M. W. (1981). Mechanism of chromosome separation during mitosis in *Fusarium (Fungi imperfecti)*. New evidence from ultrastructural and laser microbeam experiments. *J. Cell. Biol.* **91**, 446–458.
- ALLEN, E. D. AND SUSSMAN, S. (1978). Presence of an actin-like protein in mycelium of *Neurospora crassa*. *J. Bact.* **135**, 713–716.
- ANDERSON, J. M. AND SOLL, D. R. (1986). Differences in actin localization during bud and hypha formation in the yeast *Candida albicans*. *J. gen. Microbiol.* **132**, 2035–2047.
- ASHTON, M.-L. AND MOENS, P. B. (1982). Light and electron microscopy of conjugation in the yeast *Schizosaccharomyces octosporus*. *Can. J. Microbiol.* **28**, 1059–1077.
- BRODIE, H. J. (1949). *Cyathus vernicosus*, another tetrapolar bird's nest fungus. *Mycologia* **41**, 652–659.
- BUTT, T. M. AND HEATH, I. B. (1988). The changing distribution of actin and nuclear behaviour during the cell cycle of the mite-pathogenic fungus *Neozygites* sp. *Eur. J. Cell Biol.* **46**, 499–505.
- BYERS, B. AND GOETSCH, L. (1975). Behaviour of spindles and spindle plaques in the cell cycle and conjugation of *Saccharomyces cerevisiae*. *J. Bact.* **124**, 511–523.
- FUKUI, Y. (1978). Intranuclear actin bundles induced by dimethyl sulfoxide in interphase nucleus of *Dictyostelium*. *J. Cell Biol.* **76**, 146–157.
- FUKUI, Y. (1980). Formation of multinuclear cells induced by

- dimethyl sulfoxide. Inhibition of cytokinesis and occurrence of novel nuclear division in *Dictyostelium* cells. *J. Cell Biol.* **86**, 181–189.
- FUKUI, Y. AND KATSUMARU, H. (1979). Nuclear actin bundles in *Amoeba*, *Dictyostelium* and human HeLa cells induced by dimethyl sulfoxide. *Expl Cell Res.* **120**, 451–455.
- FUKUI, Y. AND KATSUMARU, H. (1980). Dynamics of nuclear actin bundle induction by dimethyl sulfoxide and factors affecting its development. *J. Cell Biol.* **84**, 131–140.
- GIRBARDT, M. (1968). Ultrastructure and dynamics of the moving nucleus. In *Aspects of Cell Motility* (ed. P. L. Miller), vol. 22, pp. 249–259. Oxford: Oxford University Press.
- HASEK, J., RUPES, I., SVOBODA, J. AND STREIBLOVA, E. (1987). Tubulin and actin topology during zygote formation of *Saccharomyces cerevisiae*. *J. gen. Microbiol.* **133**, 3355–3363.
- HEATH, I. B. (1981). Nucleus associated organelles of fungi. *Int. Rev. Cytol.* **69**, 191–221.
- HEATH, I. B. (1987). Preservation of a labile cortical array of actin filaments in growing hyphal tips of the fungus *Saprolegnia ferax*. *Eur. J. Cell Biol.* **44**, 10–16.
- HEATH, I. B. (1988). Evidence against a direct role for cortical actin arrays in saltatory organelle motility in hyphae of the fungus *Saprolegnia ferax*. *J. Cell Sci.* **91**, 41–47.
- HEATH, I. B., ASHTON, M.-L., RETHORET, K. AND HEATH, M. C. (1982). Mitosis and the phylogeny of *Taphrina*. *Can. J. Bot.* **60**, 1696–1725.
- HEATH, I. B. AND HEATH, M. C. (1978). Microtubules and organelle movements in the rust fungus *Uromyces phaseoli* var. *vignae*. *Cytobiologie* **16**, 393–411.
- HEATH, I. B. AND KAMINSKYJ, S. G. W. (1989). The organization of tip-growth-related organelles and microtubules revealed by quantitative analysis of freeze-substituted oomycete fungi. *J. Cell Sci.* **93**, 41–52.
- HEIDEMAN, S. R. AND MCINTOSH, J. R. (1980). Visualization of the structural polarity of microtubules. *Nature, Lond.* **286**, 517–519.
- HOCH, H. C. AND STAPLES, R. C. (1983). Visualization of actin in situ by rhodamine-conjugated phalloidin in the fungus *Uromyces phaseoli*. *Eur. J. Cell Biol.* **32**, 52–58.
- MCKERRACHER, L. J. AND HEATH, I. B. (1985). Microtubules around migrating nuclei in conventionally-fixed and freeze-substituted cells. *Protoplasma* **125**, 162–172.
- MCKERRACHER, L. J. AND HEATH, I. B. (1986). Fungal nuclear behaviour analysed by ultraviolet microbeam irradiation. *Cell Motil. Cytoskel.* **6**, 35–47.
- MCKERRACHER, L. J. AND HEATH, I. B. (1987). Cytoplasmic migration and intracellular organelle movements during tip growth of fungal hyphae. *Expl Mycol.* **11**, 79–100.
- MEYER, S. L. F., KAMINSKYJ, S. G. W. AND HEATH, I. B. (1988). Nuclear migration in a *nud* mutant of *Aspergillus nidulans* is inhibited in the presence of a quantitatively normal population of cytoplasmic microtubules. *J. Cell Biol.* **106**, 773–778.
- PRATT, M. M. (1989). Cytoplasmic dynein and related adenosine triphosphatases. In *Cell Movement, Volume 2: Kinesin, Dynein, and Microtubule Dynamics* (ed. F. D. Warner and J. R. McIntosh), pp. 115–124. New York: Alan R. Liss, Inc.
- RAUDASKOSKI, M. (1984). Unusual structure of nuclei in a b-mutant strain of *Schizophyllum commune* with intercellular nuclear migration. *Nord. J. Bot.* **4**, 217–233.
- RAUDASKOSKI, M. AND KOLTIN, Y. (1973). Ultrastructural aspects of a mutant of *Schizophyllum commune* with continuous nuclear migration. *J. Bact.* **116**, 981–988.
- RUNEBERG, P., RAUDASKOSKI, M. AND VIRTANEN, I. (1986). Cytoskeletal elements in the hyphae of the homobasidiomycete *Schizophyllum commune* visualized with indirect immunofluorescence and NBD-phalloidin. *Eur. J. Cell Biol.* **41**, 25–32.
- SANGER, J. W., GWINN, J. AND SANGER, J. M. (1980). Dissolution of cytoplasmic actin bundles and the induction of nuclear actin bundles by dimethyl sulfoxide. *J. exp. Zool.* **213**, 227–230.

(Received 7 August 1989 – Accepted 13 September 1989)